LOW-METALLICITY MASSIVE SINGLE STARS WITH ROTATION

B. Kubátová [a]*

[a] *Astronomical Institute of the Czech Academy of Sciences*
Fričova 298, 251 65 Ondřejov, Czech Republic

Massive low-metallicity stars are essential for understanding cosmic history. These stars are thought to be the progenitors of certain types of supernovae, gamma-ray bursts, and gravitational wave-emitting mergers. These exotic phenomena contribute to their host galaxies through intense ionising radiation and energy and momentum feedback. To better understand the nature of these stars and to quantify the feedback from them to their host galaxies, spectroscopic observations of these stars and their analyses are of great importance.

We focus on a certain type of very metal-poor (0.02 $Z_{\odot}$) hot massive single stars that rotate fast and evolve chemically homogeneously. Combining state-of-the-art theories of stellar evolution and stellar atmosphere modelling, we predict synthetic spectra and wind properties of these stars corresponding to different masses and evolutionary phases. The Hubble Space Telescope's Ultraviolet Legacy Library of Young Stars as Essential Standards (ULLYSES) project will allow us to compare our predicted spectra with observations of stars of similar nature (e.g. metal-poor stars in Sextant A).

Keywords: stars: atmospheres – stars: winds, outflows – stars: evolution – galaxies: dwarf

1. INTRODUCTION

Massive stars with low metal content (also called metal-poor stars) are essential because they provide unique insights into the earliest stages of stellar and galactic evolution, as well as the mechanisms driving the enrichment of the Universe with heavier elements. These stars are laboratories for exploring the

)https://doi.org/10.59849/2078-4163.2024.2.6
* E-mail: brankica.kubatova@asu.cas.cz

conditions and processes of the early Universe, helping us to understand star formation, galaxy evolution, cosmic reionisation and the origin of the elements. By studying them, it is possible to piece together a more complete picture of how the Universe evolved from a simple, primordial state to the complex, structured cosmos we observe today.

Massive low-metallicity stars are thought to be similar to the first stars to form after the Big Bang, known as Population III stars [1]. These stars are likely to have had very low or even zero metallicity as they formed from the primordial hydrogen and helium left over from the Big Bang. Direct observations of these stars are not possible. Today we can only observe their supernova remnants [2].

Massive stars generally emit large amounts of ultraviolet (UV) radiation, which can ionise the surrounding gas. During the "Epoch of Reionisation" [3], such radiation reionised the hydrogen in the Universe [4], ending the cosmic "dark ages" and making the Universe transparent to visible light. By studying similar massive low-metallicity stars, we can gain insight into how early massive stars may have ionised the intergalactic medium, a key process in the evolution of the Universe [5].

Massive low-metallicity stars played a key role in the formation of the first heavy elements in the Universe, such as carbon, oxygen, and nitrogen. They are primary progenitors of core-collapse supernovae [6], especially high-energy explosions, because they lose less mass to stellar winds and retain more mass until their end. Low-metallicity stars also shape the formation of the first galaxies by driving gravitational dynamics, turbulence, and feedback, with their radiation and winds influencing gas distribution and cooling [7].

Metal-poor stars are ideal progenitors of long-lived gamma-ray bursts (GRBs) and massive binary black holes (BBHs). Low metallicity minimises the angular momentum loss through winds, enabling the high rotational speeds needed for the collapsar formation, which drives GRBs [8, 9]. In addition, reduced stellar winds in metal-poor environments lead to heavier compact objects and stable close binaries, increasing the likelihood of neutron star or black hole mergers. LIGO and Virgo observations of high-mass BBHs are consistent with these expectations [10, 11].

Metal-poor stars are key to understanding the Universe, yet our limited observational capabilities prevent us from studying the first and second generations of early stars. Even nearby extremely metal-poor stars, such as those in local dwarf galaxies like Sextans A, are rarely observed and analyzed individually [12]. The spectral characteristics of stars with metallicities below $0.1Z_{\odot}$ remain largely unexplored.

The importance of studying low-metallicity stars has been underscored by the Hubble Space Telescope (HST), which has allocated 1,000 orbits to the Director's

Discretionary Time project known as the Ultraviolet Legacy Library of Young Stars as Essential Standards (ULLYSES; [13]).

1.1. ULLYSES and XShootU projects

Stars in the Large and Small Magellanic Clouds (LMC and SMC) are the primary targets observed in the ULLYSES project. These galaxies serve as ideal laboratories for studying massive stars in low-Z regions due to their proximity and metallicity levels, which are 50% and 20% of solar metallicity ($Z_{\odot}$), respectively. These unique features make them ideal targets for investigating spatially resolved populations of low-Z massive stars. A pilot study of stars with sub-SMC metallicities (10% $Z_{\odot}$) in Sextans A and NGC 3109 is also part of the ULLYSES project. ULLYSES seeks to achieve uniform coverage across all spectral subtypes from O2 to B9, while ensuring representation of all luminosity classes for spectral types O2-B1.5 at both LMC and SMC metallicities. This effort encompasses approximately 250 stars Fig. 1.

The UV part of the spectra is key for studying the iron abundance and wind parameters (e.g., terminal velocity v_{∞}) of massive stars. However, the optical wavelengths are crucial for determining stellar properties such as effective temperature ($T_{\rm eff}$), surface gravity ($\log g$), luminosity (L_*), and abundances. Reliable insights into wind clumping and mass-loss rates ($\dot{M}$) require a combination of optical and near-infrared (NIR) data. To enhance the legacy of ULLYSES, the complementary X-Shooting ULLYSES (XShootU) project was established, which provide high-quality optical and NIR spectra using the broad-wavelength X-shooter spectrograph on European Southern Observatory (ESO) Very Large Telescope (VLT; [15]), complementing UV data and extending the focus to longer wavelengths.

One of the main goals of the XShootU project [16] is to better understand the physics and evolution of low metallicity massive stars and consistently determine of stellar parameters, including $T_{\rm eff}$, $\log g$, L_*, and abundances, along with wind properties like v_{∞}, $\dot{M}$, and clumping properties as a function of metallicity. The XShootU project aims to deliver a high-quality, homogeneous optical dataset to complement ULLYSES, advancing models and understanding of massive stars in low-Z environments. These datasets are essential for the interpretation of high-Z observations with JWST/NIRSpec.

The UVB and optical X-shooter data collected by the XShootU large programme have been processed in a consistent and systematic manner. The community is provided with various higher-level data products [17]. These high-quality datasets offer lasting value for future research endeavors, including those not yet envisioned.

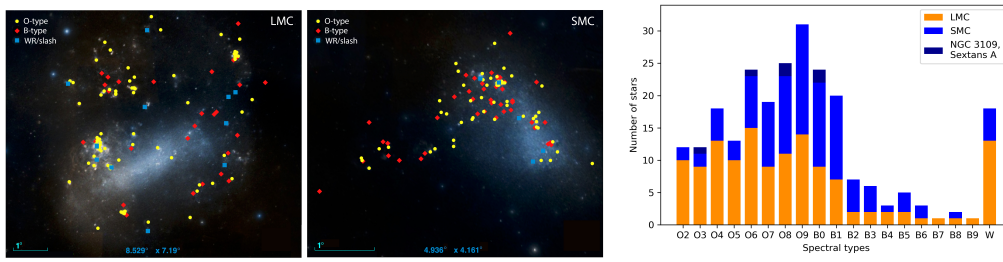

Fig. 1. *Left and middle panels*: The positions of the ULLYSES/XShootU sources in the LMC (left) and SMC (right) are shown, with yellow dots for O-type stars, red diamonds for B-type stars, and blue squares for WR and WR-like Of/WR 'slash' stars. Note the differing spatial scales. The figure uses DSS2 colour images via the Aladin Sky Atlas [14]. *Right panel*: The spectral type distribution in ULLYSES accounts only for the primary components of the ten known binaries in the sample. The category labelled "W" in the x-axes includes WR stars and WR-like "slash" stars. Courtesy: J. S. Vink [16].

2. VERY METAL-POOR MASSIVE STARS WITH ROTATION

To gain a deeper insight into very metal-poor stars, Szécsi et al. [18] modelled the evolution of single massive stars with a metallicity matching *I Zw 18* ($Z \sim 0.02, Z_{\odot}$). They found that rapidly rotating stars evolve chemically homogeneously due to rotational mixing [19] and named them Transparent Wind UV-Intense (TWUIN) stars [20]. These stars exhibit weak, optically thin winds and emit predominantly in the UV spectrum due to their high temperatures. In the Hertzsprung-Russell (HR) diagram, TWUIN stars evolve blueward during core-hydrogen burning (CHB), unlike slower-rotating or non-rotating stars, which move toward the right side of the HR diagram, similar to metal-rich massive stars in our Galaxy Fig. 2.

TWUIN stars remain theoretical predictions based on advanced stellar evolution models. To understand their spectroscopic properties and assess their impact on *I Zw 18* or other metal-poor galaxies, we analyze their spectral features, identify observable signatures, and propose a classification framework.

3. STELLAR EVOLUTIONARY MODELS

Using the 'Bonn' stellar evolution code, we calculated single stellar evolutionary tracks for fast-rotating, low-metallicity massive stars ($Z \sim 0.02\ Z_{\odot}$) during the CHB phase (for details on the code and initial parameters, we refer to [18] and references therein). To explore their hydrogen-free evolution, Szécsi et al., 2015

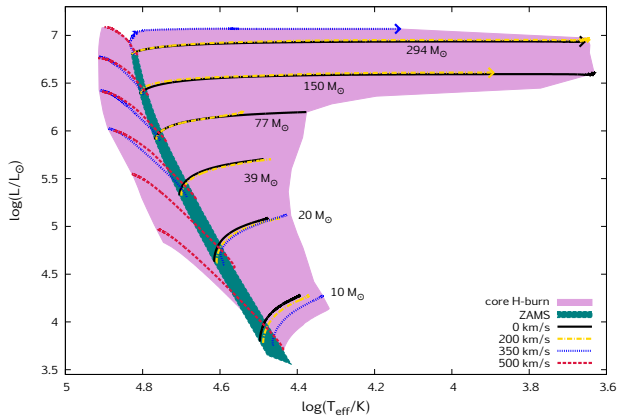

Fig. 2. The HR diagram shows evolutionary tracks during CHB for models with initial masses of 9–300 $M_{\odot}$ and rotational velocities of 0–500 km/s, at 1/10 Z_{SMC} metallicity. The purple region marks the CHB phase, while the green region indicates the zero-age main sequence (ZAMS). CHB stars are expected on both sides of the ZAMS within the purple region, with arrows marking incomplete tracks. Courtesy:D. Szécsi [18].

[20] extended these tracks into the core-helium-burning (CHeB) phase, following them until helium exhaustion in the core.

To represent different evolutionary stages through spectra, we use three chemically homogeneous tracks with initial masses ($M_{\rm ini}$) of 20, 59, and 131 $M_{\odot}$ and rotational velocities of 450 km/s, 300 km/s, and 600 km/s, respectively (see Fig. 1 in [21]). These sequences assume a fast initial rotation, inherited by the 15 models we compute spectra for. Their rotational velocities range between $400-1000$ km/s (see Table 1 in [21]), which remains well below the critical limit for massive stars ($\sim\ 0.4-0.6\ v_{crit}$), ensuring no formation of decretion disks. For each initial mass, five models were computed: four representing the CHB phase with surface helium mass fractions (Y_S) of 0.28, 0.5, 0.75, and 0.98, and one representing the CHeB phase with a central helium mass fraction (Y_C) of 0.1. Further details on these models and their evolutionary tracks can be found in Table 1 and Fig. 1 of [21].

Different mass-loss rate prescriptions were applied depending on the evolutionary stage. For $Y_S < 0.55$, the Vink et al. (2001, [22]) mass-loss rate prescription for hot O-type stars (see e.g. 24 in their paper) was used. For $Y_S > 0.7$, we adopted the WR-type prescription from [23], scaled down by a factor of 10 as suggested by [24]. Throughout the entire CHeB phase, the WR-type prescription was consistently applied.

To address uncertainties in the mass-loss rate predictions, we calculated two sets of synthetic spectra for each model: one using the nominal mass-loss rates

from the evolutionary models, and another with mass-loss rates reduced by a factor of 100. This reduction factor was chosen based on evidence that the WR wind metallicity dependence might be steeper [25]. The values of both the nominal and reduced mass-loss rates used in our computations are given in Table 2 of [21].

4. STELLAR ATMOSPHERE AND WIND MODELS

To calculate synthetic spectra and determine wind parameter stratification, we used the Potsdam Wolf-Rayet (`PoWR`) atmosphere code [26,27]. This code models both the quasi-static (photospheric) and expanding (wind) layers of stellar atmospheres, solving the non-LTE radiative transfer in a spherically expanding atmosphere with stationary mass outflow. The radiation field and population numbers are iteratively solved using statistical equilibrium and radiative transfer equations in the comoving frame. The temperature stratification is updated iteratively to ensure energy conservation, using the electron thermal balance method [28] and a generalised Unsöld-Lucy method assuming radiative equilibrium [29]. Line profiles are treated as Gaussians with a Doppler broadening velocity of $v_{\rm D} = 100$ km/s, accounting for thermal and microturbulent velocities. Once the model converges, the emergent spectrum is calculated in the observer's frame using detailed atomic data and accounting for thermal, microturbulent, and pressure broadening.

To account for all significant contributors to opacity, the spectra calculations included key elements such as H, He, C, N, O, Ne, Mg, Al, Si, and Fe, with their abundances derived from stellar evolutionary model sequences. Additional elements not included in these models, such as P, S, Cl, Ar, and K, were incorporated in the `PoWR` code with abundances set to $Z_{\odot}/50$ to account for their potential impact on wind driving. The wind density stratification, ρ(r), was determined using the mass continuity equation, $\dot{M} = 4\pi r^2 v(r)\rho(r)$, with the mass-loss rate taken from the evolutionary models. The velocity stratification $v(r)$ followed the so so-called β-law, $v(r) = v_{\infty}(1 - R_*/r)^{\beta}$ [30], with β set to 0.8 or 1.0 and v_{∞} assumed to be 1000 km/s for all models. Wind inhomogeneities (clumping) were modelled using the microclumping approximation [31], assuming optically thin clumps, a void inter-clump medium, and a radius-dependent clumping factor (D, [32]). To assess the impact of clumping on the spectra of metal-poor massive stars, we generated two sets of synthetic spectra: one assuming a smooth wind with D=1, and the other using D=10.

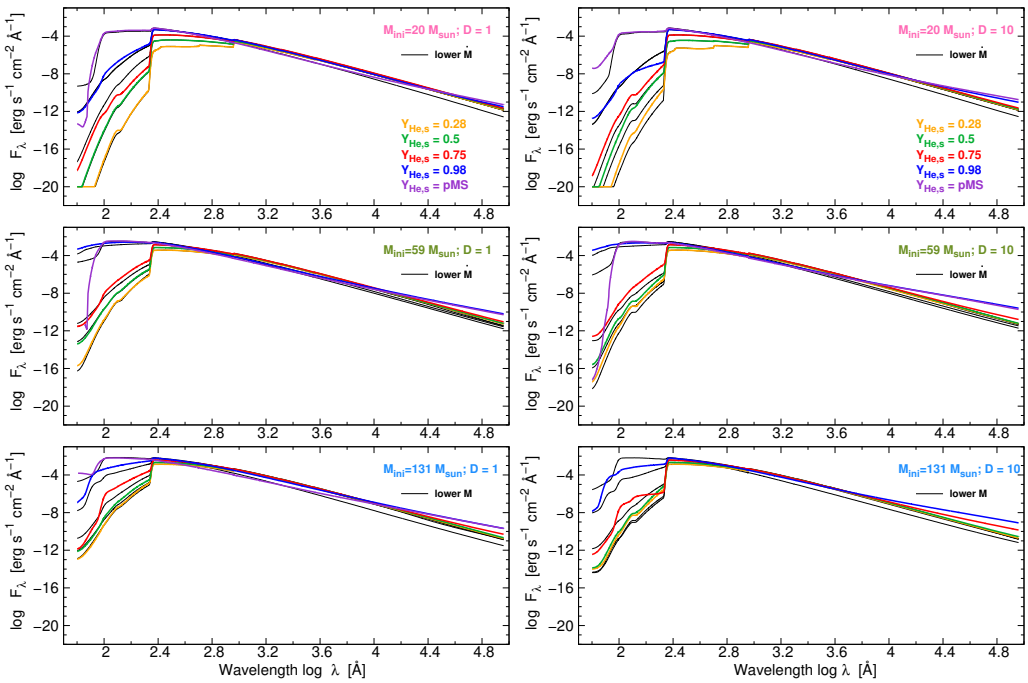

Fig. 3. The continuum SEDs of chemically homogeneous stars are shown for different initial masses (M_{ini}), noted in the top-right corner of each panel) and evolutionary stages (Y_S, indicated in the top-left panel). The coloured lines represent models calculated with nominal mass-loss rates (as used in the stellar evolutionary models) and smooth winds (D=1) on the left panels and clumped winds (D=10) on the right panels. The black lines show the SEDs for the same models but with mass-loss rates reduced by a factor of 100.

5. RESULTS

We calculated a total of 60 models for stars undergoing chemically homogeneous evolution. These models were based on three different initial masses (M_{ini}), five evolutionary stages defined by the helium fraction (Y_S), and two variations in mass-loss rates and wind clumping. The line profiles were computed while accounting for the effects of radiation damping, pressure broadening, and rotational broadening.

5.1. Spectral characteristics

For each model, we calculated the spectral energy distribution (SED) and found that chemically homogeneous stars emit most of their radiation in the far- and extreme-UV regions. The total flux emitted by these stars is not highly sensitive to changes in mass-loss rates or wind clumping. However, small differences

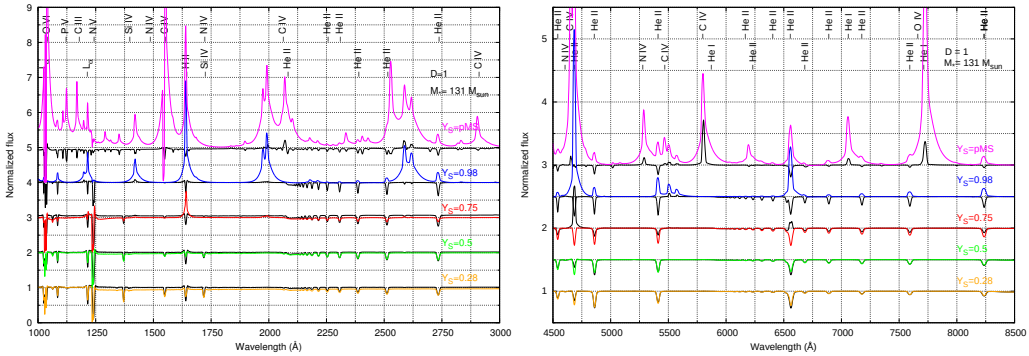

Fig. 4. The synthetic spectra of chemically homogeneous stars with an initial mass of $M_{ini} = 131\ M_{\odot}$ are shown for the UV (left panel) and optical (right panel) regions at different evolutionary stages, indicated by the Y_S values. The coloured lines represent models using the nominal mass-loss rates (as adopted in the stellar evolutionary models) with smooth winds (D=1). In contrast, the black lines show the same models but with mass-loss rates reduced by a factor of 100.

in the SEDs appear at wavelengths shorter than 227 Å and longer than 10 000 Å, especially during the late main sequence ($Y_S = 0.98$) and post-main sequence (CHeB) phases (see Fig. 1). The SEDs also show that radiation with frequencies higher than the ionisation limits of H I, He I, and He II increases with both the star's initial mass and its evolutionary progress. This indicates that more massive and evolved stars emit stronger ionising flux.

In the earlier evolutionary stages ($Y_S < 0.5$), the synthetic spectra primarily show absorption lines, regardless of the star's initial mass. As the stars evolve, emission lines begin to appear, becoming dominant during the CHeB phase, where the spectra resemble those of Wolf-Rayet (WR) stars. Strong helium emission lines are a notable feature during this phase (see Fig. 4).

Based on these spectral features, chemically homogeneous stars in their early phases can be categorised as TWUIN stars, characterised by weak, optically thin winds. In later phases, they develop features typical of WR stars, with strong, optically thick winds (see purple lines in Fig. 4). Detailed spectral calculations in the UV, in the optical and in the infrared wavelength range can be seen in the figures 3, 4, 6 and in the appendix of [21].

5.2. Spectral classification

Using the Morgan-Keenan spectroscopic classification scheme, we assigned spectral classes to the synthetic spectra of chemically homogeneous stars. During the core hydrogen-burning (CHB) phase, these stars exhibit spectra corresponding to spectral class O4 or earlier, with luminosity classes I (supergiant), III (giant),

or V (dwarf). The spectra are characterised by strong He II emission lines and an almost complete absence of metal lines. In this phase, these stars are predicted to be significantly hotter than any O-type stars observed so far, even at metallicities as low as 0.1 $Z_{\odot}$).

As the stars evolve into the CHeB phase, they evolve into WO-type WR stars, where ionised oxygen dominates their spectra. These stars' spectra lack nitrogen lines entirely. For more details on the spectral classification, refer to Table 4 and Appendix A in [21].

Due to the limited spectroscopic data available for individual massive stars with metallicities below 0.1$\sim Z_{\odot}$, we couldn't compare our spectra with observations of similar stars. The primary goal of our study was to encourage future observational efforts targeting low-metallicity star-forming galaxies, such as Sextans A or I Zwicky 18.

6. ACKNOWLEDGEMENTS

This work was supported by a grant GA ČR 22-34467S. The Astronomical Institute Ondřejov is supported by the project RVO: 67985815.

REFERENCES

1. Klessen, R. S. & Glover, S. C. O., 2023, AJ, **61**, 65-130
2. Xing, Q.-F., Zhao, G., Liu, Z.-W., et al., 2023, Nature, **618**, 7966
3. Furlanetto, S., Carilli, C., Mirocha, J., et al., 2019, Bull. Am. Astron. Soc., **51**, 3
4. Abel, T., Bryan, G. L., Norman, M. L., 2002, Science, **295**, 5552
5. Freundlich, J., 2024, Fundamental Plasma Physics, **11**, 100059
6. Smartt, S. J., 2009, Annual Review of A&A, **47**, 1
7. Geen, S., Rosdahl, J., Blaizot, J., et al., 2015, MNRAS, **448**, 4
8. Levesque, E. M., Kewley, L. J., Berger, E., Zahid, H. J., 2010, AJ, **140**, 5
9. Vergani, S. D., Salvaterra, R., Japelj, J., 2015, A&A, **581**, A102
10. Abbott, B. P., Abbott, R., Abbott, T. D., et al., 2016, Ap.J. Letters, **18**, 2
11. Abbott, B. P., Abbott, R., Abbott, T. D., et al., 2017, Phys. Rev. Letters, **118**, 22
12. Garcia, M., Herrero, A., Najarro, F., et al., 2019, MNRAS, **484**, 1

13. Roman-Duval, J., Proffitt, C. R., Taylor, J. M., et al., 2020, Res. Notes Am. Astron. Soc., **4**, 205

14. Bonnarel, F., Fernique, P., Bienaymé, O., et al., 2000, A&AS, **143**, 33-40

15. Vernet, J., Dekker, H., D'Odorico, S., et al. 2011, A&A, **536**, A105

16. Vink, J. S., A. Mehner, P. A. Crowther, et al., 2023, A&A, **675**, A154.

17. Sana, H., Tramper, F., Abdul-Masih, M., et al., 2024, A&A, **688**, A104

18. Szécsi, D., Langer, N., Sanyal, D., et al., 2015, A&A, **581**, A15

19. Maeder, A., 1987, A&A, **178**

20. Szécsi, D., 2016, PhD thesis, Mathematisch Naturwissenschaftlichen Fakultät der Universität Bonn

21. Kubátová, B., Szécsi, D., Sander, A. A. C., et al., 2019, A&A, **623**, A8

22. Vink, J., de Koter, A., Lamers, H., 2001, A&A, **369**, 574

23. Hamann, W.-R., Koesterke, L., Wessolowski, U., 1995, A&A, **299**, 151

24. Yoon, S.-C., Langer, N., Norman, C., 2006, A&A, **460**,

25. Hainich, R., Pasemann, D., Todt, H., et al., 2015, A&A, **581**, A21

26. Hamann, W.-R. & Gräfener, G., 2004, A&A, **427**, 697

27. Sander, A., Shenar, T., Hainich, R., et al., 2015, A&A, **577**, A13

28. Kubát, J., Puls, J., & Pauldrach, A. W. A., 1999, A&A, **341**, 587

29. Hamann, W.-R., & Gräfener, G. 2003, A&A, **410**, 993

30. Lamers, H., & Cassinelli, J., 1999, Introduction to Stellar Winds (Cambridge University Press)

31. Hamann, W.-R., & Koesterke, L., 1998, A&A, **335**, 1003

32. Sander, A. A. C., Hamann, W.-R., Todt, H., et al., 2017, A&A, **60**, A86